

X-ray Absorption Fine Structure Spectroscopic Studies of Octakis(DMSO)lanthanoid(III) Complexes in Solution and in the Solid Iodides

Ingmar Persson,^{*†} Emiliana Damian Risberg,[‡] Paola D'Angelo,[§] Simone De Panfilis,[£] Magnus Sandström,^{*‡} and Alireza Abbasi^{‡,||}

Department of Chemistry, Swedish University of Agricultural Sciences, P.O. Box 7015, SE-750 07 Uppsala, Sweden, Department of Physical, Inorganic and Structural Chemistry, Stockholm University, SE-106 91 Stockholm, Sweden, Dipartimento di Chimica, Università di Roma "La Sapienza", Piazzale Aldo Moro 5, I-00185 Roma, Italy, European Synchrotron Radiation Facility (ESRF), BP 220, 38043 Grenoble Cedex, France, and School of Chemistry, University College of Science, University of Tehran, P.O. Box 14155-6455, Tehran, Iran

Received April 5, 2007

Octakis(DMSO)lanthanoid(III) iodides (DMSO = dimethylsulfoxide), $[\text{Ln}(\text{OS}(\text{CH}_3)_2)_8]\text{I}_3$, of most lanthanoid(III) ions in the series from La to Lu have been studied in the solid state and in DMSO solution by extended X-ray absorption fine structure (EXAFS) spectroscopy. L_3 -edge and also some K-edge spectra were recorded, which provided mean Ln–O bond distances for the octakis(DMSO)lanthanoid(III) complexes. The agreement with the average of the Ln–O bond distances obtained in a separate study by X-ray crystallography was quite satisfactory. The crystalline octakis(DMSO)lanthanoid(III) iodide salts have a fairly broad distribution of Ln–O bond distances, ca. 0.1 Å, with a few disordered DMSO ligands. Their EXAFS spectra are in excellent agreement with those obtained for the solvated lanthanoid(III) ions in DMSO solution, both of which show slightly asymmetric distributions of the Ln–O bond distances. Hence, all lanthanoid(III) ions are present as octakis(DMSO)lanthanoid(III) complexes in DMSO solution, with the mean Ln–O distances centered at 2.50 (La), 2.45 (Pr), 2.43 (Nd), 2.41 (Sm), 2.40 (Eu), 2.39 (Gd), 2.37 (Tb), 2.36 (Dy), 2.34 (Ho), 2.33 (Er), 2.31 (Tm), and 2.29 Å (Lu). This decrease in the Ln–O bond distances is larger than expected from the previously established ionic radii for octa-coordination. This indicates increasing polarization of the $\text{Ln}^{\text{III}}\text{--O}(\text{DMSO})$ bonds with increasing atomic number. However, the S(1s) electron transition energies in the sulfur K-edge X-ray absorption near-edge structure (XANES) spectra, probing the unoccupied molecular orbitals of lowest energy of the DMSO ligands for the $[\text{Ln}(\text{OS}(\text{CH}_3)_2)_8]^{3+}$ complexes, change only insignificantly from Ln = La to Lu. This indicates that there is no appreciable change in the σ -contribution to the S–O bond, probably due to a corresponding increase in the contribution from the sulfur lone pair to the bonding.

Introduction

The series of the highly charged lanthanoid(III) ions provides unique possibilities to study the chemical bonding in similar complexes, comparing the effect of a regular decrease in ionic size with increasing atomic number on the

coordination of ligands with the same type of donor atom. In addition, the Ln–O bond distances for a series with a specified coordination number in the solid state provide useful comparisons with complexes in solution. For aqueous solutions, a proposed sudden transition from the hydration number nine to eight with decreasing size in the series of lanthanoid(III) ions, the “gadolinium break”, has been debated for an extended period of time.^{1,2} The significance of the “gadolinium break” in terms of structural changes will

* To whom correspondence should be addressed. E-mail: ingmar.persson@kemi.slu.se (I.P.).

† Swedish University of Agricultural Sciences.

‡ Stockholm University.

§ Università di Roma “La Sapienza”.

£ European Synchrotron Radiation Facility.

|| University of Tehran.

(1) Abbasi, A.; Lindqvist-Reis, P.; Eriksson, L.; Sandström, D.; Lidin, S.; Persson, I.; Sandström, M. *Chem. Eur. J.* **2005**, *11*, 4065–4077.

be discussed in a separate paper on the hydrated lanthanum(III) ions.³

Changes in coordination number have been proposed to take place in other oxygen-donor solvents. The Ln–O distances of the solvated lanthanoid(III) ions in oxygen-coordinating solvents have been reported to decrease continuously in the series from lanthanum(III) to lutetium(III), e.g., from 2.49 to 2.30 Å in *N,N*-dimethylformamide and from 2.47 to 2.22 Å in *N,N*-dimethylacetamide.⁴ For *N,N*-dimethylformamide, all coordination numbers were found to be close to eight, while continuously decreasing coordination numbers in the range from 8.5 to 6.5 were reported for the *N,N*-dimethylacetamide series.⁴ However, the data analyses of those extended X-ray absorption fine structure (EXAFS) spectra were not performed with modern methods and the accuracy of the results seems doubtful. For crystalline lanthanoid(III) solvates of the bulky oxygen-donor ligand *N,N'*-dimethylpropyleneurea, recent results reveal a coordination number of six throughout the lanthanoid series, while in solution the increase in the mean Ln–O distance shows that the coordination number becomes seven for all lanthanoid(III) ions except for the smallest one, lutetium(III), which is hexa-coordinated.⁵ Evidently, ligand–ligand interactions, the size of the lanthanoid(III) ion and the nature of the Ln–O bonds are important factors for the coordination number and geometry, and are in the present work studied for the DMSO solvates.

Dimethyl sulfoxide (DMSO) is a very efficient solvent for electrolytes because of its high dipole moment, $\mu = 3.96$ D, and high permittivity, $\epsilon = 46.4$. The electron-pair donor ability ($D_S = 27.5$) is higher than that for water ($D_S = 17$),⁶ and DMSO is sterically more demanding as a ligand. For the fully DMSO-solvated lanthanoid(III) ions all crystal structures reported show discrete octakis(DMSO)lanthanoid(III) complexes, e.g., in the iodide, bromide, and perchlorate salts, often with disordered DMSO ligands.^{7–14}

All octakis(DMSO)lanthanoid(III) iodides display a distribution of Ln–O bond distances with alternative positions for at least one of the ligands.¹⁴ The difficulty to unambiguously determine the mean Ln–O bond distances due to the disorder in the crystal structures prompted an EXAFS study, which is lattice-independent and provides a mean of the M–O bond distances. The current EXAFS study also encompasses DMSO solutions of the lanthanoid(III) ions. In this way, reliable comparisons of bond distances between crystalline solvates and corresponding solutions were enabled.

Sulfur K-edge X-ray absorption near edge structure (XANES) spectroscopy has previously turned out to be sensitive to changes in bond character, when applied to the hexakis(DMSO) solvates of the trivalent ions in Group 13, aluminum(III), gallium(III), indium(III), and thallium(III),¹⁵ and was applied here on the series of octakis(DMSO)-lanthanoid(III) complexes.

Experimental Section

Crystalline Samples and Solutions. Crystalline octakis(DMSO)lanthanoid(III) iodides, $[\text{Ln}(\text{OS}(\text{CH}_3)_2)_6]_3$ (Ln = La, Ce, Pr, Nd, Sm, Gd, Tb, Dy, Ho, Er, Tm, and Lu), were prepared as described in the preceding paper.¹⁴ Ca. 0.2 mol·dm⁻³ solutions were prepared by dissolving the solid solvates in DMSO (Aldrich), freshly distilled over calcium hydride (Fluka) under reduced pressure.

EXAFS Data Collection. L₃-edge data, and in some cases K-edge data (for La, Gd, Er, and Lu), were collected. The K-edge measurements were performed at the bending magnet beamline BM29 at the European Synchrotron Radiation Facility (ESRF), Grenoble, France,¹⁶ which was operated at 6.0 GeV in 16-bunch mode and a maximum current of 80 mA. The L₃-edge measurements were performed at the wiggler beam line 4-1 and the bending magnet beamline 2-3 at the Stanford Synchrotron Radiation Laboratory (SSRL), Stanford, CA, which was operated at 3.0 GeV and a maximum current of 100 mA, and at beamline I811 at MAX-lab, Lund University, Sweden, operated at 1.5 GeV and a maximum current of 200 mA. The EXAFS stations at ESRF, SSRL, and MAX-lab were equipped with Si[511], Si[220], and Si[111] double-crystal monochromators, respectively. At SSRL, monochromator crystals with different cuts were selected to reduce disturbing monochromator glitches. Higher-order harmonics were reduced by detuning the second monochromator crystal to reflect 80% of maximum intensity at the K-edges, and 30–50% of maximum intensity at the L₃-edges (less for lower energy) at the end of the scans. At the L₃-edges, simultaneous data collection was performed when possible both in transmission using ion chambers and in fluorescence mode with a Lytle detector¹⁷ with appropriate filters and a very gentle argon flow. For transmission measurements, the solids were diluted with boron nitride to provide an approximate edge step of about one unit in the logarithmic intensity ratio. An energy-discriminating Ge detector showed that fluorescence from the iodide ions contributed to increase the background intensity for the low-energy measurements. For the DMSO solvates of lanthanum(III)¹⁸ and neodymium(III), trifluoromethanesulfonate salts were also used without any significant change in the mean

- (2) Richens, D. T. *The chemistry of aqua ions*; John Wiley and Sons: New York, 1997.
- (3) D'Angelo, P.; Persson, I.; Sandström, M.; Abbasi, A.; Lundberg, D. Unpublished results.
- (4) Ishiguro, S.; Umebayashi, Y.; Kato, K.; Takahashi, R.; Ozutsumi, K. *J. Chem. Soc., Faraday Trans.* **1998**, *94*, 3607–3612.
- (5) Lundberg, D. The coordination chemistry of solvated metal ions in DMPU, Ph.D. Thesis, Swedish University of Agricultural Sciences, Uppsala, Sweden, 2006.
- (6) Sandström, M.; Persson, I.; Persson, P. *Acta Chem. Scand.* **1990**, *44*, 653–675.
- (7) Chan, E. J.; Cox, B. G.; Harrowfield, J. M.; Ogden, M. I.; Skelton, B. W.; White, A. H. *Inorg. Chim. Acta* **2004**, *357*, 2365–2373.
- (8) Zhang, Q.-F.; Leung, W.-H.; Xin, X.-Q.; Fun, H.-K. *Inorg. Chem.* **2000**, *39*, 417–426.
- (9) (a) Cherkasova, T. G. *Zh. Neorg. Khim.* **1994**, *39*, 1316–1319. (b) Cherkasova, T. G.; Anosova, Yu. V.; Shevchenko, T. M. *Zh. Neorg. Khim.* **2004**, *49*, 22–25.
- (10) Plotnikova, T. E.; Grigor'ev, M. S.; Fedoseev, A. M.; Antipin, M. Yu. *Russ. J. Coord. Chem.* **2004**, *30*, 60–67.
- (11) Huang, Q.; Wu, X.; Lu, J. *Chem. Commun.* **1997**, 703–704.
- (12) Klinga, M.; Cuesta, R.; Moreno, J. M.; Dominguez-Vera, J. M.; Colacio, E.; Kivekäs, R. *Acta Crystallogr., Sect C* **1998**, *54*, 1275–1277.
- (13) Sivapullaiah, P. V.; Soundararajan, S. *Current Sci.* **1975**, *44*, 374–376.
- (14) Abbasi, A.; Damian Risberg, E.; Eriksson, L.; Mink, J.; Persson, I.; Sandström, M.; Sidorov, Y. V.; Skripkin, M. Yu.; Ullström, A.-S. *Inorg. Chem.* **2007**, *46*, 7731–7741.

- (15) Damian, E.; Jalilehvand, F.; Abbasi, A.; Pettersson, L. G. M.; Sandström, M. *Phys. Scr.* **2005**, *T115*, 1077–1079.
- (16) Filipponi, A.; Borowski, M.; Bowron, D. T.; Ansell, S.; Di, Cicco, A.; De Panfilis, S.; Itié, J.-P. *Rev. Sci. Instrum.* **2000**, *71*, 2422–2432.
- (17) <http://www.exafsc.com/products/3-grid-detector.html>
- (18) Näslund, J.; Lindqvist-Reis, P.; Persson, I.; Sandström, M. *Inorg. Chem.* **2000**, *39*, 4006–4011.

Ln–O bond distances. Other difficulties, especially pronounced for the light lanthanoid(III) ions, are the restricted k -range before the onset of the L_2 absorption edge, and the frequent multiple excitation features after the L_3 -edge, at ca. $k = 6 \text{ \AA}^{-1}$.¹⁹ The noise level of the K -edge data was generally somewhat higher, and the short core–hole lifetime, τ_{h} , in the high-energy range ($\Gamma = 14.1$ and 33.7 eV giving $\tau_{\text{h}} = 4.7 \times 10^{-17}$ and $2.0 \times 10^{-17} \text{ s}$ for La and Lu, respectively) causes a damping and broadening of the signal, which in particular affects the high-frequency components of the measured signal, and consequently reduces the sensitivity of the technique of the more distant coordination shells.²⁰ Nevertheless, the large k -range, the low absorption allowing transmission measurements, and the absence of glitches and double excitations are clear advantages when comparing with the data collected in the L_3 -edge regions of the light lanthanoid(III) ions. The difference in the information obtained from K - and L_3 -edges is discussed in a separate paper.²⁰

EXAFS Data Analysis. For each sample, 3–4 scans were averaged by means of the EXAFSPAK program package,²¹ after energy calibrations performed by measuring appropriate metal foils, simultaneously if possible, otherwise before and after the scans. The EXAFSPAK and GNXAS²² program packages were both used for the data treatment. In the first case, standard procedures were applied for pre-edge subtraction and spline removal.²² The GNXAS code is based on the calculation of the entire EXAFS signal with a simultaneous refinement of the structural parameters.²³ The GNXAS method accounts for multiple scattering (MS) paths, with correct treatment of the configurational average of all the MS signals to allow fitting of correlated distances and bond distance variances (Debye–Waller factors). To account for asymmetry in the distribution of the ion–solvent distances,²⁴ the Ln–O two-body signals associated with the first coordination shells were modeled with Γ -like distribution functions, which depend on four parameters, namely the coordination number, N , the average distance, R , the mean-square variation, σ^2 , and the skewness, β . R is the first moment of the function $4\pi \int g(r)^2 dr$, where R is the average (centroid) distance and not the position of the maximum of the distribution (R_{m}). An asymmetric distribution of Ln–O distances can be accounted for also by introducing a cumulant expansion of the effective distribution function, where the third cumulant, C_3 , in the expansion will contribute to the XAFS phase and therefore influence the determination of the mean distance. Note that the β parameter is related to the third cumulant C_3 through the relation $C_3 = \beta\sigma^3$. The amplitude reduction factor, S_0^2 , was refined in all calculations, and the refined values were very close to 1 for all systems.

The error limits in the refined parameters in Table 1 are estimated from the variations in the results using different data programs and data ranges for the modeling and analysis procedures, also

considering the shift in the E_0 value (for which $k = 0$). The accuracy, including systematic errors, of the distances obtained for the separate complexes is within $\pm 0.02 \text{ \AA}$ for well-defined interactions.

XANES. Sulfur K -edge XANES spectra were recorded in fluorescence mode at the SSRL beam line 6-2, in the same way as previously reported.¹⁵ The X-ray energy scale was calibrated by setting the lowest energy peak of sodium thiosulfate ($\text{Na}_2\text{S}_2\text{O}_3 \cdot 5\text{H}_2\text{O}$) to 2469.2 eV .²⁵ The spectral features correspond to transitions from the $1s$ orbital of the sulfur atom to unoccupied molecular orbitals (MO:s) with a significant contribution of sulfur $3p$.

Results and Discussion

EXAFS Measurements. The interpretation of the current EXAFS data of the lanthanoid(III) series involves some special concerns in particular for the lighter elements, e.g., the restricted L_{III} EXAFS k -range containing additional absorption features due to double electron excitations, high absorption in fluorescence mode, the added background fluorescence from the iodide, and the asymmetry caused by the distribution of the distances within a coordination shell. For these reasons, principally the GNXAS program was employed, which handles multiple scattering and double excitations in a more rigorous way and also made it possible to treat some fluorescence data with particularly difficult splining to extract the EXAFS oscillation. In GNXAS, the spline was calculated and applied together with the structural parameters of the model. In Table 1, the results are reported from the GNXAS evaluations allowing for asymmetry, and in the Supporting Information, results from GNXAS without asymmetry are compared with a standard EXAFSPAK treatment without asymmetry and with removal of double excitations by a deglitching procedure.

All the recently determined crystal structures of the octakis(DMSO) lanthanoid(III) iodides, $[\text{Ln}(\text{OS}(\text{CH}_3)_2)_8]\text{I}_3$ (Ln = La, Ce, Pr, Nd, Sm, Gd, Dy, Er, and Lu), show a distribution of the Ln–O bond distances within a range of about 0.1 \AA .¹⁴ The crystallographic Ln–O average has an inherently different weighting than the mean Ln–O bond distance obtained for the same solid compound from the EXAFS data, where bonds with high Debye–Waller (disorder) parameters contribute less than shorter and more distinct distances.

The larger k -range for the K -edge EXAFS data is more favorable for evaluating asymmetry in the Ln–O distributions (Table 1) than the restricted k -range of the L_3 -edge (Figure 1). Already direct comparisons of the almost identical EXAFS spectra and Fourier transforms (Figures 1 and 2) indicate that there are no significant differences between the structures of the DMSO-solvated lanthanoid(III) ions in the solid state and in solution. The X-ray absorption spectra are plotted from $k = 0$ to show that also the near edge XANES region is very similar in all cases, even though the k -range used in the calculations normally starts at $k \approx 3 \text{ \AA}^{-1}$.

In all analyses, by means of different programs with or without allowing for asymmetry for the Ln–O distribution,

(19) Solera, J. A.; García, J.; Proietti, M. G. *Phys. Rev. B* **1995**, *51*, 2678–2686.

(20) D'Angelo, P.; De Panfilis, S.; Filipponi, A.; Persson, I. Unpublished results.

(21) George, G. N.; Pickering, I. J. *EXAFSPAK, A Suite of Computer Programs for Analysis of X-ray Absorption Spectra*; SSRL, Stanford University: Stanford, CA, 1993.

(22) Filipponi, A.; Di Cicco, A. GNXAS: A Software Package for Advanced EXAFS Multiple-Scattering Calculations and Data-Analysis. *Task Q.* **2000**, *4*, 575–669.

(23) Filipponi, A.; Di Cicco, A.; Natoli, C. R. *Phys. Rev. B* **1995**, *52*, 15122–15134. Filipponi, A.; Di Cicco, A. *Phys. Rev. B* **1995**, *52*, 15135–15149.

(24) Crozier, E. D.; Rehr, J. J.; Ingalls, R. In *X-ray absorption; Principles, Applications, Techniques of EXAFS, SEXAFS and XANES*; Koningsberger, D. C., Prins, R., Eds.; John Wiley and Sons: New York, 1988; Chapter 9.

(25) Sekiyama, H.; Kosugi, N.; Kuroda, H.; Ohta, T. *Bull. Chem. Soc. Jpn.* **1986**, *59*, 575–589.

Table 1. EXAFS Structural Parameters of the Octakis(DMSO)lanthanoid(III) Complexes in the Solid State and in DMSO Solution, as Determined by GNXAS^a

		K-edge data			L ₃ -edge data		
		Ln–O	S–O	Ln···S/∠Ln–O–S	Ln–O	S–O	Ln···S/∠Ln–O–S
[La(OS(CH ₃) ₂) ₈]I ₃ (s)	<i>d</i>	2.507 (2.484)	1.54	3.69/130	2.486 (2.465)	1.53	3.73/135
	σ^2/C_3	0.0073/2.56 × 10 ⁻⁴	0.0029	0.010	0.0045/1.62 × 10 ⁻⁴	0.0025	0.0145
La ³⁺ /Me ₂ SO	<i>d</i>	2.503 (2.493)	1.51	3.72/135	2.497(2.484)	1.51	3.69/132
	σ^2/C_3	0.0086/4.1 × 10 ⁻⁵	0.0019	0.016	0.012/7.4 × 10 ⁻⁵	0.0020	0.015
[Ce(OS(CH ₃) ₂) ₈]I ₃ (s)	<i>d</i>				2.465 (2.465)	1.53	3.77/141
	σ^2/C_3				0.0040/<1 × 10 ⁻⁶	0.0026	
[Pr(OS(CH ₃) ₂) ₈]I ₃ (s)	<i>d</i>				2.452 (2.444)	1.52	3.611/130
	σ^2/C_3				0.0080/4.6 × 10 ⁻⁵	0.0018	0.012
Pr ³⁺ /Me ₂ SO	<i>d</i>				2.457/2.450	1.54	3.714/135
	σ^2/C_3				0.0098/1.8 × 10 ⁻⁵	0.0013	0.011
[Nd(OS(CH ₃) ₂) ₈]I ₃ (s)	<i>d</i>				2.434 (2.426)	1.53	3.608/130
	σ^2/C_3				0.0060/2.4 × 10 ⁻⁵	0.0016	0.0117
Nd ³⁺ /Me ₂ SO	<i>d</i>				2.431(2.427)	1.53	3.606/130
	σ^2/C_3				0.0127/1.6 × 10 ⁻⁵	0.0006	0.022
[Sm(OS(CH ₃) ₂) ₈]I ₃ (s)	<i>d</i>				2.414 (2.404)	1.53	3.603/131
	σ^2/C_3				0.0086/4.6 × 10 ⁻⁵	0.0023	0.020
Sm ³⁺ /Me ₂ SO	<i>d</i>				2.412 (2.406)	1.54	3.607/131
	σ^2/C_3				0.0050/2.1 × 10 ⁻⁵	0.0018	0.012
Eu ³⁺ /Me ₂ SO	<i>d</i>				2.400 (2.394)	1.53	3.622/133
	σ^2/C_3				0.0053/2.3 × 10 ⁻⁵	0.0020	0.011
[Gd(OS(CH ₃) ₂) ₈]I ₃ (s)	<i>d</i>	2.391 (2.383)	1.51	3.562/130	2.395 (2.385)	1.52	3.591/133
	σ^2/C_3	0.0059/2.5 × 10 ⁻⁵	0.0015	0.0096	0.010/2.4 × 10 ⁻⁵	0.0023	0.013
Gd ³⁺ /Me ₂ SO	<i>d</i>	2.388 (2.381)	1.53	3.570/130	2.388 (2.381)	1.529	3.580/131
	σ^2/C_3	0.0063/2.1 × 10 ⁻⁵	0.0015	0.0099	0.0080/3.2 × 10 ⁻⁵	0.0024	0.011
[Tb(OS(CH ₃) ₂) ₈]I ₃ (s)	<i>d</i>				2.370 (2.363)	1.53	3.553/131
	σ^2/C_3				0.0073/2.3 × 10 ⁻⁵	0.0020	0.0098
Tb ³⁺ /Me ₂ SO	<i>d</i>				2.367 (2.363)	1.54	3.571/131
	σ^2/C_3				0.0086/1.7 × 10 ⁻⁵	0.0013	0.0094
[Dy(OS(CH ₃) ₂) ₈]I ₃ (s)	<i>d</i>				2.362 (2.353)	1.52	3.520/129
	σ^2/C_3				0.0077/3.0 × 10 ⁻⁵	0.0011	0.0094
Dy ³⁺ /Me ₂ SO	<i>d</i>				2.361 (2.352)	1.52	3.535/130
	σ^2/C_3				0.0080/3.5 × 10 ⁻⁵	0.0016	0.0106
Ho ³⁺ /Me ₂ SO	<i>d</i>				2.337 (2.329)	1.53	3.538/131
	σ^2/C_3				0.0089/2.3 × 10 ⁻⁵	0.0015	0.0102
[Er(OS(CH ₃) ₂) ₈]I ₃ (s)	<i>d</i>	2.326 (2.320)	1.51	3.464/128	2.333 (2.326)	1.51	3.498/130
	σ^2/C_3	0.0064/0.88 × 10 ⁻⁵	0.0013	0.0089	0.0045/2.6 × 10 ⁻⁵	0.0014	0.0067
Er ³⁺ /Me ₂ SO	<i>d</i>	2.331 (2.324)	1.51	3.453/127	2.337 (2.331)	1.51	3.542/133
	σ^2/C_3	0.0071/2.2 × 10 ⁻⁵	0.0019	0.0100	0.0060/2.2 × 10 ⁻⁵	0.0016	0.0078
[Tm(OS(CH ₃) ₂) ₈]I ₃ (s)	<i>d</i>				2.313 (2.308)	1.55	3.517/130
	σ^2/C_3				0.0059/1.2 × 10 ⁻⁵	0.0024	0.0083
Tm ³⁺ /Me ₂ SO	<i>d</i>				2.316 (2.311)	1.55	3.540/132
	σ^2/C_3				0.0078/0.44 × 10 ⁻⁵	0.0019	0.0087
[Lu(OS(CH ₃) ₂) ₈]I ₃ (s)	<i>d</i>	2.300 (2.292)	1.53	3.445/127	2.294 (2.293)	1.53	3.497/131
	σ^2/C_3	0.0076/3.8 × 10 ⁻⁵	0.0023	0.0070	0.0060/0.11 × 10 ⁻⁵	0.0022	0.0081
Lu ³⁺ /Me ₂ SO	<i>d</i>	2.297 (2.287)	1.53	3.464/129	2.288 (2.282)	1.51	3.504/134
	σ^2/C_3	0.0072/3.2 × 10 ⁻⁵	0.0012	0.0081	0.0055/2.8 × 10 ⁻⁵	0.0020	0.011

^a The centroid Ln–O distance (*d* in Å), the disorder parameter σ^2 (Å²), the third cumulant *C*₃ (Å³), and (within parentheses) the peak maximum of the asymmetric distribution of Ln–O bond distances, *R*_m (Å). The S–O bond distance (Å), obtained for a Gaussian distribution of bond distances, and the Ln–O–S bond angle (deg) have also been refined. The number of distances is fixed to eight for all systems.

the variations in the bond distances do not exceed 0.02 Å for the same type of sample. Furthermore, the peak value *R*_m of the Ln–O distribution is not more than 0.01 Å below the centroid value, *d*, of the asymmetry model (Table 1). The Debye–Waller parameters $\sigma^2_{\text{Ln–O}}$, which fall rather consistently between 0.005 and 0.010 Å², and the small third cumulant parameters, *C*₃, show that the distributions of the Ln–O bond distances are fairly wide but not very asymmetric. Comparisons of the Fourier transforms for the L₃- and K-edge spectra with the model spectra are shown for some of the samples in Figure 2. The agreement is satisfactory in all cases.

The weighted mean of the EXAFS values obtained for the Ln–O distances of each solid and of the corresponding

solution is in Table 1 compared to the average value obtained from the crystal structure determinations.¹⁴ The plot in Figure 3 shows some minor deviations, e.g., the ~0.015 Å lower value for the crystal structure of praseodymium and the similarly higher values for erbium, thulium, and lutetium, which probably reflect the difficulty to model the disordered DMSO ligands. However, the mean Ln–O bond distances obtained are in all cases shorter than those expected from combining tabulated ionic radii for eight-coordination,²⁶ with the effective oxygen radius 1.34 Å derived for coordinated water;²⁷ the latter value has been found to be applicable also

(26) Shannon, R. D. *Acta Crystallogr., Sect A* **1976**, *32*, 751–767.

(27) Beattie, J. K.; Best, S. P.; Skelton, B. W.; White, A. H. *J. Chem. Soc., Dalton Trans.* **1981**, 2105–2011.

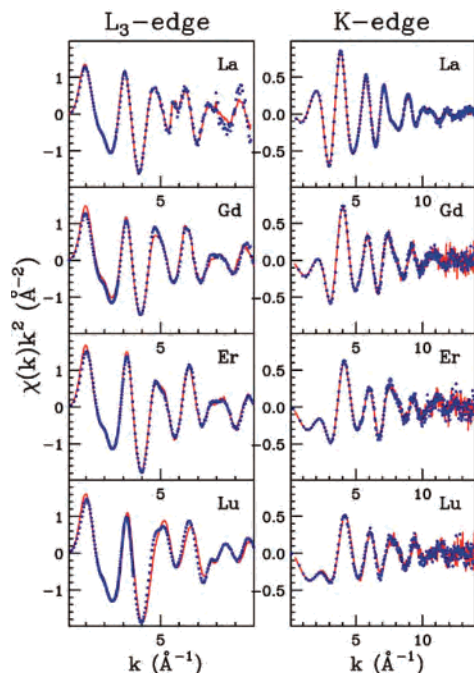


Figure 1. L_{3-} and K-edge EXAFS spectra for some Ln(III) ions in DMSO solution (blue dots), compared with corresponding EXAFS spectra of the solid $[\text{Ln}(\text{OS}(\text{CH}_3)_2)_8]\text{I}_3$ compounds (red lines).

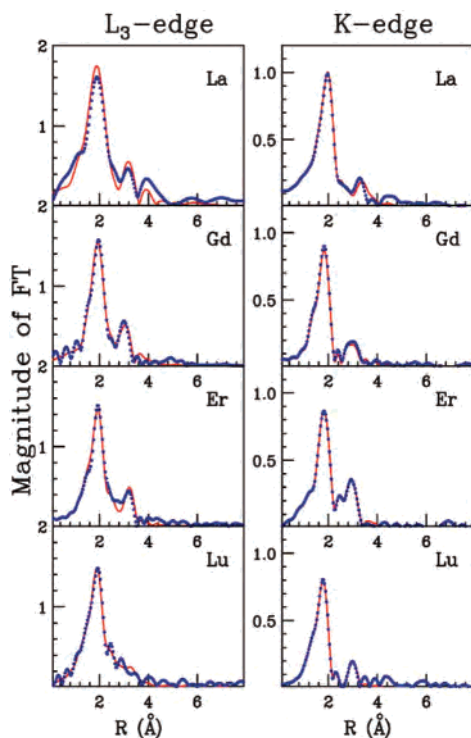


Figure 2. Fourier transforms of the calculated (red lines) and experimental (blue dots) EXAFS spectra of some selected lanthanoid(III) ions in DMSO solution at the L_{3-} and K-edges.

for the DMSO oxygen in several comparative studies.^{18,28,29} The ionic radii of the lanthanoid(III) ions, derived from rare earth fluorides for eight-coordination, decrease from 1.16 Å for lanthanum(III) to 0.98 Å for lutetium(III), Figure 3 and Table S2.²⁶

The deviation in the Ln–O bond distance from the sum of ionic radii increases for the heavier elements (cf. Figure

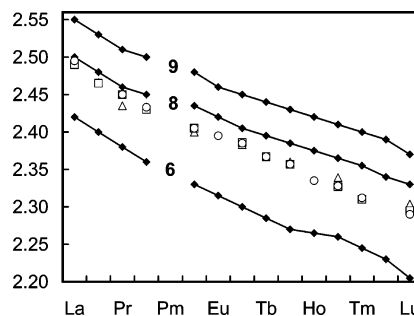


Figure 3. Mean Ln–O bond distances (Å) for $[\text{Ln}(\text{OS}(\text{CH}_3)_2)_8]^{3+}$ complexes as obtained with EXAFS (this study) in solution (O) and in the solid state (□), and crystallographically (Δ) (ref 14). The lines display the sum of the tabulated ionic radii of the lanthanoid(III) ions for 9-, 8-, and 6-coordination (ref 26) and the oxygen radius 1.34 Å (ref 27).

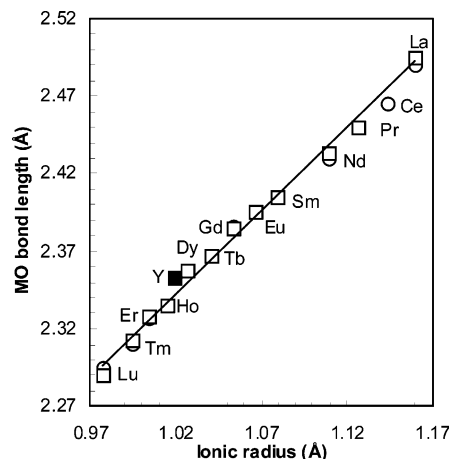


Figure 4. Correlation between Ln–O bond distances for $[\text{Ln}(\text{OS}(\text{CH}_3)_2)_8]^{3+}$ complexes (solid iodides O, DMSO solution □), obtained by EXAFS (this study), and ionic radii for eight-coordination (ref 26). For yttrium(III), the bond distance 2.36 Å is obtained from ref 29.

3, Table S2), probably because the gradually increasing electrostatic interaction for those smaller, highly charged ions polarizes the Ln–O bonds. The linear correlation between the Ln–O bond distances and ionic radii in Figure 4 indicates that the systematic deviation in Figure 3 is due to a gradual decrease in the apparent radius of the coordinated DMSO oxygen atom with decreasing size of the lanthanoid(III) ions. The distribution of the Ln···S distances in an $[\text{Ln}(\text{OS}(\text{CH}_3)_2)_8]^{3+}$ complex is expected to be even wider than that for the Ln–O distances and is consistent with the somewhat higher disorder (σ^2) parameters (Table 1). However, the Ln···S distances could only be modeled as a Gaussian distribution, resulting in an uncertain mean Ln–O–S angle that does not show the expected decreasing tendency with increasing atomic number as clearly as for the crystal structures.¹⁴

The model refinements in the GNXAS program yield a value for the S–O bond distance, which is a minor

(28) Näslund, J.; Persson, I.; Sandström, M. *Inorg. Chem.* **2000**, *39*, 4012–4021. Kristiansson, O.; Persson, I.; Bobicz, D.; Xu, D. *Inorg. Chim. Acta* **2003**, *344*, 15–27. Ullström, A.-S.; Warminska, D.; Persson, I. *J. Coord. Chem.* **2005**, *58*, 611–622; D'Angelo, P.; Chillemi, G.; Barone, V.; Mancini, G. Sanna, N.; Persson, I. *J. Phys. Chem. B* **2005**, *109*, 9178–9185.

(29) Lindqvist-Reis, P.; Näslund, J.; Persson, I.; Sandström, M. *J. Chem. Soc., Dalton Trans.* **2000**, *16*, 2703–2710.

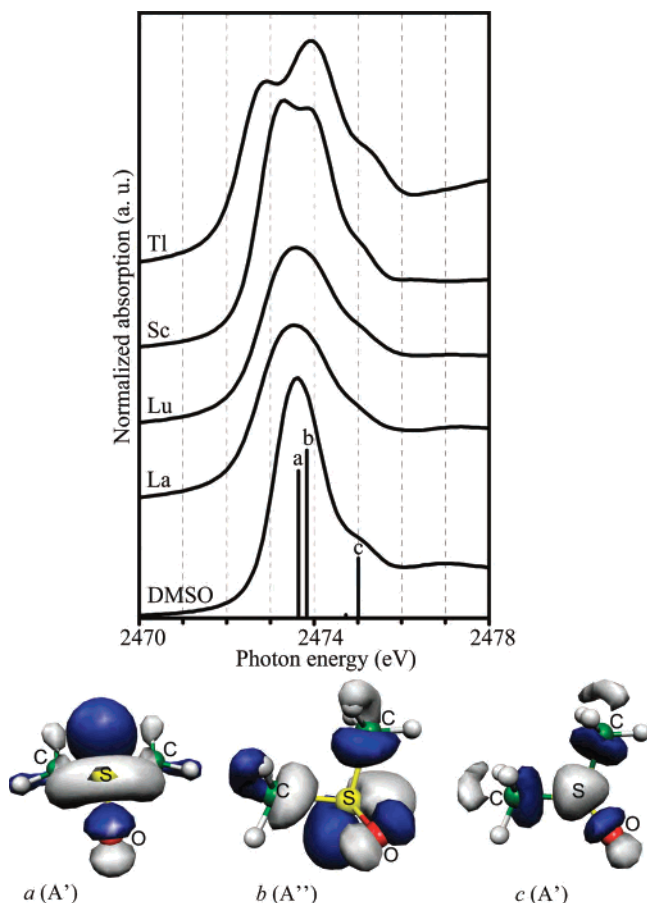


Figure 5. (upper) Normalized sulfur K-edge XANES spectra of DMSO-solvated ions: the hexasolvates of thallium(III) (transition energies from second derivative at 2472.7, 2474.0, and 2475.4 eV) and scandium(III) (2473.1, 2474.0, and 2475.2 eV), the octasolvates of lutetium(III) (2473.3 and 2475.2 eV) and lanthanum(III) (2473.3 and 2475.1 eV), and 0.05 M DMSO in acetonitrile (2473.6 and 2475.2 eV); the S(1s) electron transitions calculated for the uncoordinated DMSO molecule are denoted *a*, *b*, and *c* (vertical bars, cf. ref 15). (below) Electron density contours of the receiving MO:s (different colors for different phases) for the three main S(1s) transitions *a*, *b*, and *c* show antibonding σ^* , π^* , and σ^* character for the S–O bond, respectively.

contribution and to some extent reflects the data quality. The S–O bond has partial double-bond character, and its bond length increases for O-bonded DMSO ligands. In a comprehensive survey, the mean S–O bond distance of oxygen-coordinated solvates was found to be 1.528(1) Å,³⁰ consistent with an average of the currently obtained values, which vary between 1.51 and 1.55 Å with a small σ^2 parameter, from 0.001 to 0.003 Å² (Table 1).

Sulfur XANES. The sulfur K-edge XANES spectra in Figure 5 for the crystalline DMSO solvates of the trivalent ions thallium(III), scandium(III), lutetium(III), and lanthanum(III) are compared with 0.05 M DMSO in acetonitrile solution. The asymmetric peak in the XANES spectrum of the DMSO molecule contains three transitions from S(1s) labeled *a*, *b*, and *c*, as shown by previous analyses by transition potential DFT computations.¹⁵ The shapes of the receiving MO:s have been visualized by the program

MOLEKEL.³¹ Transition *a* corresponds to an MO with character of antibonding $\sigma^*(\text{S–O})$ plus S lone pair, *b* mainly antibonding $\pi^*(\text{S–O})$, and *c* antibonding $\sigma^*(\text{S–O}, \text{S–C})$.

The previous experimental and theoretical study of the sulfur K-edge XANES spectra of the $[\text{M}(\text{OS}(\text{CH}_3)_2)_6]^{3+}$ solvates of the trivalent Group 13 ions, M = Al, Ga, In, and Tl, showed that the energy and spectral intensity of transition *a* was particularly affected for the hexakis(DMSO) thallium(III) solvate.¹⁵ Also, the comparison in Figure 5 indicates that the metal–oxygen bonding may in the first place shift transition *a* toward low energy while transitions *b* and *c* are less affected. However, the coordination of DMSO to a lanthanoid(III) ion seems to have little influence on the receiving molecular orbitals. All sulfur K-edge XANES spectra for the octakis(DMSO)lanthanoid(III) complexes in this study showed very similar shape (the spectra for La at the beginning and Lu at the end of the series are shown in Figure 5) with the asymmetric absorption peak only slightly broader than that for unsolvated DMSO molecules in dilute acetonitrile solution. For the small lanthanoid-like ion scandium(III) in its six-coordinated DMSO solvate, the energy of transition *a* decreased somewhat further (Figure 5) and is fairly similar to that in the $[\text{Al}(\text{OS}(\text{CH}_3)_2)_6]^{3+}$ solvate of the even smaller Al(III) ion, which also has a d⁰ electronic configuration (cf. Figure 2 in ref 15).

Vibrational spectroscopy is another probe of changes in the metal ion–oxygen bonding, especially useful for DMSO complexes, because correlations can also be made with the intramolecular S–O bonds. Previous analyses of the vibrational force constants for the dimethyl-solvated trivalent ions (cf. Figures 4, 5 in ref 14) show that the M–O stretching force constants ($K_{\text{M–O}}$) vary relatively little in the lanthanoid(III) series and also for the solvated Group 3 ions, Sc(III), Y(III), and La(III), despite a large change in their mean M–O bond distance. The force constants $K_{\text{S–O}}/K_{\text{M–O}}$ (in N cm^{−1}) for the DMSO solvates in Figure 5 are La(III) 4.545/1.432; Lu(III) 4.691/1.496;¹⁴ Sc(III) 4.402/1.462;³² and Tl(III), 4.279/1.300.³³ Corresponding values for Y(III) are 4.677/1.490,¹⁴ Al(III), 4.599/1.761; Ga(III), 4.168/1.617; In(III), 4.274/1.318;³³ while $K_{\text{S–O}}$ for a gaseous DMSO molecule is 5.061 N cm^{−1}.³²

An M(III)–O bond is expected to increase the charge difference between the O and S atoms and induce a σ -electron transfer from the sulfur to the oxygen atom (increasing the participation of the sulfur lone pair in the bonding) but also, depending on the metal ion, reduce the π -electron transfer from oxygen to sulfur. Therefore, a shorter and stronger M–O bonding interaction does not necessarily show a direct correlation with a weaker S–O bond, at least not when comparing their stretching force constants.

The XANES spectra in Figure 5 show that the change in ionic size in the lanthanoid(III) series does not influence the

(30) Calligaris, M. *Coord. Chem. Rev.* **2004**, *248*, 351–375. Calligaris, M.; Carugo, O. *Coord. Chem. Rev.* **1996**, *153*, 83–154.

(31) *Molekel Visualization Package*, version 4.3; <http://www.cscs.ch/molekel/manual/help.html>.

(32) Skripkin, M. Yu.; Lindqvist-Reis, P.; Abbasi, A.; Mink, J.; Persson, I.; Sandström, M. *Dalton Trans.* **2004**, 4038–4049.

(33) Molla-Abbassi, A.; Skripkin, M. Yu.; Kritikos, M.; Persson, I.; Mink, J.; Sandström, M. *Dalton Trans.* **2003**, 1746–1753.

receiving molecular orbitals localized on sulfur enough to have any significant influence on the transition energies, consistent with the small variation in the K_{S-O} stretching force constant, only 3.1% in the lanthanoid(III) series.¹⁴ The effect on the XANES spectra of the Ln–O bond when compared to that of gaseous DMSO resembles more an electrostatic interaction (point charge) than a covalent M–O bond.¹⁵ On the other hand, it seems that the splitting in the XANES spectra (decrease in transition energy from S(1s) to *a*) generally increases for comparable systems when the K_{S-O} value decreases. Since the experimentally probed receiving molecular orbital for transition *a* contains an antibonding combination of sulfur and oxygen atomic orbitals, $\sigma^*(S-O)$, such a decrease in transition energy should mean that the energy difference between the antibonding and the bonding combination, $\sigma(S-O)$, i.e., its counterpart in a covalent bond, also has decreased. This signifies a weaker σ -contribution to the S–O bond, which is compatible with the lower K_{S-O} force constant when the π -contribution to the bond remains similar.

Conclusions

The mean M–O bond distances obtained from EXAFS data for the solid octakis(DMSO) lanthanoid(III) iodides, $[Ln(OS(CH_3)_2)_8]I_3$, are in satisfactory agreement with the average values previously determined crystallographically, even for complexes modeled with up to three disordered ligands in the crystal structures. The mean Ln–O bond distances gradually decrease with increasing atomic number for the lanthanoid(III) complexes. The decreasing size of the lanthanoid(III) ions from Ln = La to Lu evidently increases the polarization of the Ln^{III}–O bond for the series of $[Ln(OS(CH_3)_2)_8]^{3+}$ complexes. However, the S(1s) transition energies to the lowest unoccupied molecular orbitals of the DMSO ligands, which were probed by sulfur K-edge XANES spectra, show insignificant changes from Ln = La to Lu. The energy range for the main S(1s) transitions is only slightly broader than that for uncoordinated DMSO. The effect on the sulfur K-edge XANES spectra for the series of $[Ln(OS(CH_3)_2)_8]^{3+}$ complexes resembles more that of an electrostatic interaction with the oxygen atom of the DMSO ligand than that of a covalent bond. Complexes of other trivalent metal ions often show significantly lower transition energy of the first main transition with antibonding $\sigma^*(S-O)$ character. Correlations with vibrational force constants indicate that in similar M–O bonding conditions the lowering of the energy of the first main transition can be used qualitatively to follow changes in the σ -contribution to the S–O bond, which is likely to involve an increased contribution of the sulfur lone pair.

The analyses of the EXAFS data for the solvated lanthanoid(III) ions in solution result in the mean Ln–O distances 2.50 (La), 2.45 (Pr), 2.43 (Nd), 2.41 (Sm), 2.40 (Eu), 2.39 (Gd), 2.37 (Tb), 2.36 (Dy), 2.34 (Ho), 2.33 (Er), 2.31 (Tm),

and 2.29 Å (Lu). Those centroid values of the Ln–O bond distances increased only slightly (<0.01 Å) when a third cumulant allowing for a phase shift in the EXAFS oscillation due to asymmetry was introduced. The mean Ln–O distances, disorder, σ^2 , and asymmetry parameters, C_3 , for the DMSO solutions are similar for the corresponding $[Ln(OS(CH_3)_2)_8]I_3$ compounds and show fairly symmetrical distributions of the Ln–O bond distances, which in the crystal structures span over about 0.1 Å. Thus, the solvated lanthanoid(III) ions in solution have similar octa-coordination as that in the solid state, as also is evident from their almost identical EXAFS spectra and Fourier transforms for both the Ln K- and L₃-edges, Figures 1 and 2. Those mean M–O bond distances decrease faster than expected from the established ionic radii for octa-coordination and approach for the heavy lanthanoid(III) ions distances expected for hepta-coordination. There is, however, no indication of a coordination number change in this series of DMSO-solvated lanthanoid(III) ions in solution, which probably reflects the flexibility and polarizability of the valence electrons in the M–O–S bonding system. For the DMSO-solvated lanthanoid-like ions of Group 3, however, transitions from the coordination number eight for the yttrium(III) ion to six for the smaller scandium(III) ion, occur both in solution and in the solid iodides, with bond distances Y–8O 2.36 and 2.34 Å^{14,29} and Sc–6O 2.085 and 2.075 Å,³² respectively.

Acknowledgment. We gratefully acknowledge the financial support by the Swedish Research Council, and the allocation of beam-time and laboratory facilities by the European Synchrotron Radiation Facility (ESRF), Stanford Synchrotron Radiation Laboratory, SSRL, Stanford, CA, and the MAX-lab, Lund University, Lund, Sweden. SSRL is a national user facility operated by Stanford University on behalf of the U.S. Department of Energy, Office of Basic Energy Sciences. The SSRL Structural Molecular Biology Program is supported by the Department of Energy, Office of Biological and Environmental Research, and by the National Institutes of Health, National Center for Research Resources, Biomedical Technology Program. The MAX-lab is supported by the Swedish Research Council and the Knut och Alice Wallenbergs Stiftelse. Additional support was obtained from Crafoordska Stiftelsen and the Faculty of Science & Technology, Norwegian University of Science & Technology.

Supporting Information Available: Table with EXAFS structural parameters of the octakis(DMSO)lanthanoid(III) complexes in the solid state and in DMSO solution, as determined by GNXAS and EXAFSPAK for Gaussian distributions of bond distances, a table with a summary of Ln–O bond distances in DMSO-solvated complexes, ionic radii of octa-coordinated lanthanoid(III) ions, and figures showing the fit of the experimental raw data. This material is available free of charge via the Internet at <http://pubs.acs.org>.

IC700659U